Thin and thick dielectric films for THz surface plasmon control

Q.1 **M M Nazarov[1,2], E A Bezus[3] and A P Shkurinov[2]**

[1] Institute on laser and Information Technologies RAS, Shatura, Moscow region 140700, Russia
[2] MV Lomonosov Moscow State University, Moscow 119992, Russia
[3] Image Processing Systems Institute of the Russian Academy of Sciences, Samara 443001, Russia

E-mail: maxim@lasmed.phys.msu.ru

Abstract
Propagation of a broadband ($\lambda = 0.3$–3 mm) THz surface plasmon (SP) through a long transparent slab of thickness d varying from $d \ll \lambda$ through $d \approx \lambda$ to $d \gg \lambda$ is experimentally studied and theoretically analyzed. It is demonstrated that the temporal and spectral shapes of the transmitted SP pulse differ considerably for those three regimes of plasmon–layer interaction. Optimal dielectric film thickness (20 μm) for SP confinement without much attenuation and dispersion is estimated.

Q.2 (Some figures may appear in colour only in the online journal)

1. Introduction

Dielectric-loaded plasmonic surfaces have attracted considerable interest in recent years in the visible frequency range [1–3]. A thin layer of transparent dielectric on the surface of the metal can significantly increase the transverse mode localization also in the highly demanded THz frequency range [4]. At low frequencies, surface plasmons (SP) suffer from high radiation losses because the SP normalized propagation constant n_{SP} is very close to the refractive index of the dielectric medium ($n_{SP} \approx 1$ in case of air), leading to weak surface confinement [5]. The slow decay of the wave into the dielectric medium is not the only consequence of $n_{SP} \approx 1$, also, the phase velocity of SP is almost equal to that of the waves propagating in free space. Therefore, power can be transferred back and forth between the two waves if they are allowed to co-propagate along the interface, which makes the investigation of THz SP challenging. This is highlighted by the fact that discrepancies up to 1–2 orders of magnitude between the attenuation length predicted from theory and experimental investigations have been reported for THz SP [5, 6]. A highly delocalized nature of this wave, low sensitivity to surface properties and significant radiation losses at bends limit practical applications of THz SP. In the present work, we try to improve SP confinement in a broad THz frequency range by adding a dielectric layer. The transmission of THz plasmonic pulses through dielectric slabs of finite length is studied.

From the measured data, we extract the SP normalized propagation constant (mode effective refractive index) n_{SP} with the employed time-domain technique. Since the THz SP refractive index n_{SP} is almost equal to unity, a slight increase in n_{SP} of about 1% is enough to confine SP to the surface and to decrease the penetration depth into the dielectric media, δ_z, defined as the distance from the surface at which the field amplitude decays by a factor of e [7] (figure 1). For the case of uncovered metal, the SP penetration depth into air is of the order of $\delta_z = 2$–5 mm.

The SP short pulse propagation through a transparent slab of thickness d is experimentally studied and theoretically analyzed for slab thicknesses varying from $d \ll \lambda$ through $d \approx \lambda$ to $d \gg \lambda$, where $\lambda = 300~\mu$m is the free-space wavelength at the central frequency of 1 THz.

2. Experimental setup and samples

As an emitter of THz radiation, an InAs surface illuminated by femtosecond pulses of Ti:Sa laser was used [8]. The generated free-space THz radiation is converted into a surface plasmon wave by the prism coupling technique [9] in the Otto configuration. The efficiency (3–10%) and bandwidth
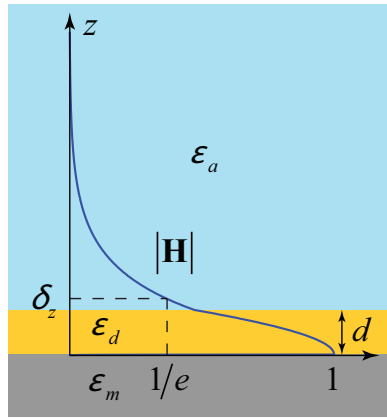
Figure 1. Field distribution of a plasmonic mode in a three-layer structure (air–dielectric film–metal). The **H** field is plotted, the **E** field has a similar distribution, but with discontinuities at air–dielectric and dielectric–metal interfaces.

(0.1–1.2 THz) of SP excitation are controlled by the air gap size (figure 2(a)), the optimal thickness of which is of the order of 0.3–1 mm [10]. In the THz frequency range, an 'artifact' free-space wave always accompanies the SP wave propagating on an uncovered metal surface [5], regardless of the excitation method. To minimize the influence of this wave, we use a metal screen located 1 mm above the surface. The studied sample is placed on the uncovered metal surface area between the coupling prism and the metal screen (figure 2(a)). Transmitted SP is then decoupled into a free-space wave on a right-angle edge of the aluminum plate and reaches the detector.

A photoconductive antenna with a pair of lenses was utilized as a detector of the THz radiation. The standard technique of terahertz time-domain spectroscopy [11] allowed us to measure the temporal shape of short pulses (figures 4–6) with and without the dielectric sample. The SP transmission spectra are evaluated after the Fourier transform and after normalization by the reference spectrum (see figure 2(b)). In contrast to the well-developed THz-TDS systems, we use surface waves for incidence and propagation through the sample. As the reference wave, SP propagating along the uncovered metal surface is used [10].

The studied films are polymer (polyethylene—LDPE, polypropylene—PP and Teflon—PTFE) slabs with $n_d = \sqrt{\varepsilon_d} \approx 1.44$, $a < 2$ cm^{-1} [12] and different height ($d = 20$–5000 μm) and length ($L = 8$–50 mm) attached to the metal surface in a fixed position between x_1 and x_2 regions, as shown in figure 2(a).

Since both the prism gap (1 mm) and the slit width (1 mm) limit the SP field in the z direction, the SP transmission amplitude depends on the x position of the film relative to the prism and to the detector. We fixed $x_1 = 10$ mm and $x_2 = 30$ mm (see figure 2(a)) for all presented measurements. For different L values, the excitation prism was moved parallel to the metal plate together with the incident THz beam, preserving all sizes and angles.

3. Results and discussion

The experimental spectra of the SP effective refractive index and absorption coefficient are presented in figure 3. The data are calculated as follows: $n_{\mathrm{SP}}(f) = 1 + \arg[T(f)] \cdot [c/(2\pi f L)]$, $\alpha_{\mathrm{SP}}(f) = -\ln[|T(f)|]/L$, where f is the radiation frequency, $T(f) = E_{\mathrm{sample}}/E_{\mathrm{ref}}$, E_{sample} is the SP spectra after transmission through a film (with length L and thickness d) attached to the metal plate, E_{ref} is the reference SP spectra
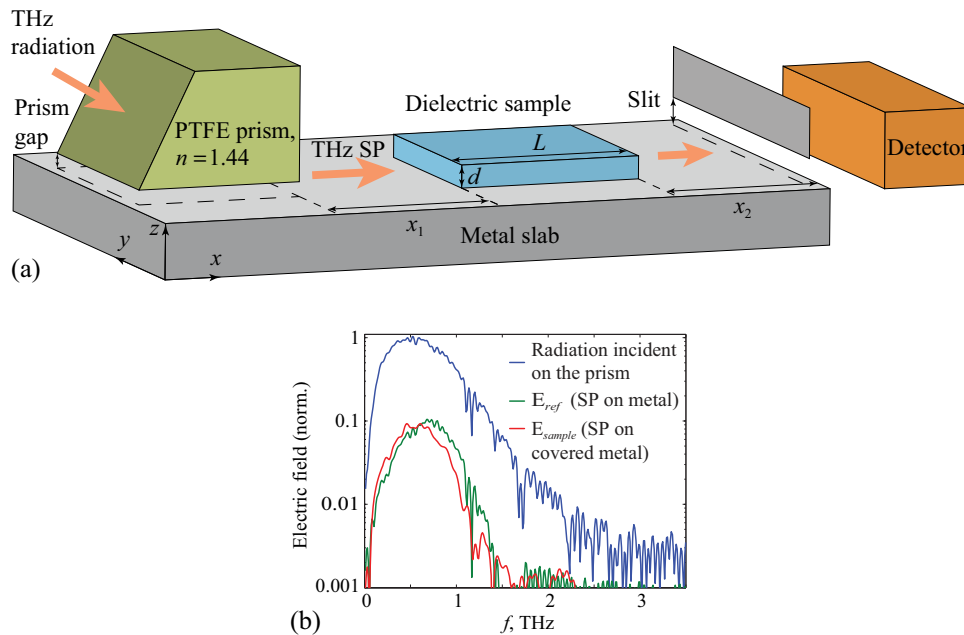

Figure 2. (a) Sketch of the experimental setup and (b) spectra of THz radiation: incident on the prism; converted into SP and propagated on Al; SP propagated on Al covered by a dielectric film with thickness $d = 20$ μm. Gap size is 0.5 mm, slit size is 2 mm, $L = 2$ cm.
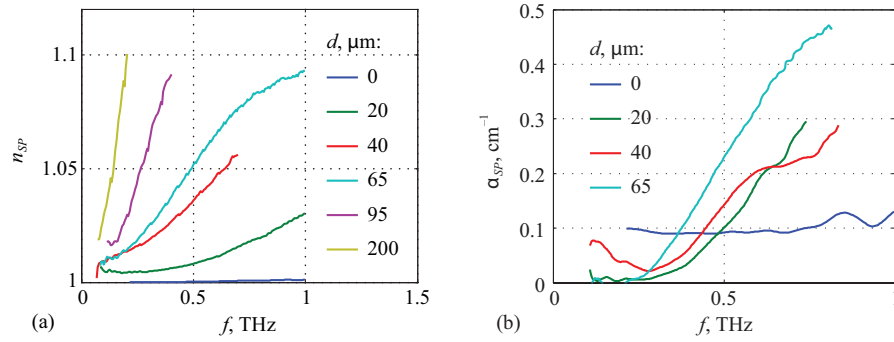
Figure 3. (a) Measured SP effective refractive index spectra for different film thickness values. (b) SP absorption coefficient spectra for different film thickness values. The film material is LDPE for $d < 200$ μm and PP for $d \geq 200$ μm, $d = 0$ indicates uncovered metal.
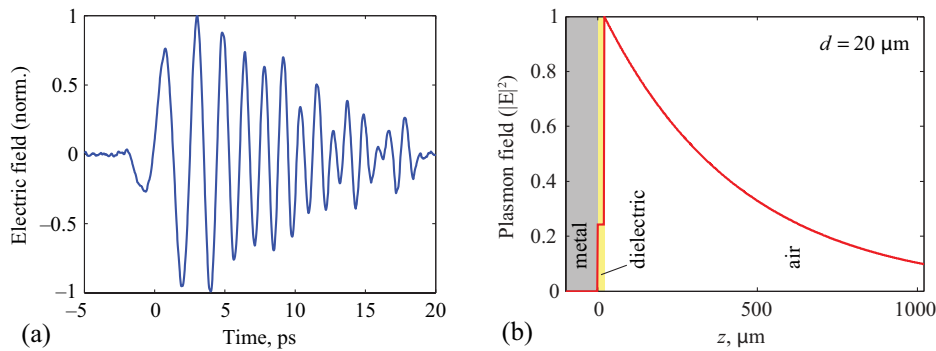

Figure 4. Plasmon pulse on a thin ($h = 20$ μm) film with $L = 80$ mm. (a) Temporal profile. Here and below $t = 0$ corresponds to the reference pulse maximum on time-domain plots. (b) Calculated electric field distribution for 0.5 THz frequency.

measured for the case $L = 0$, that is, the SP incident on the dielectric block. Let us note that the expression for $n_{SP}(f)$ given above is based on the assumption that the phase of the transmitted signal is completely determined by the properties of the plasmonic mode inside the dielectric block. The validity of this assumption is discussed below.

In accordance with previous studies [5, 10], we observe that the SP refractive index (figure 3(a)) increases with frequency f and with thickness d on a dielectric-loaded surface.

As to the absorption (figure 3(b)), it has a non-monotonic dependence on d and f. When a thin dielectric film is placed on the uncovered metal surface, the overall transmitted SP signal increases (figure 2(b)). It corresponds to an increase in SP transmission at low frequencies (figure 2(b)), so if we use SP spectra after propagation of the same distance L along the uncovered metal surface as a reference, we will obtain $T(f) > 1$. We attribute this transmission enhancement to a decrease in the SP radiation losses affecting the reference signal. When n_{SP} is larger than 1 (because of the film presence), radiation losses must disappear, the remaining losses being the scattering losses at the boundaries of the dielectric slab and the absorption inside the dielectric. Indeed, the radiation losses affect the reference wave propagating along the uncovered metal surface (where $n_{SP} \approx 1$), and not the SP signal in the dielectric film.

To measure the SP absorption and refraction on the uncovered metal ($d = 0$ case), we need another type of

reference. For that case, we consider $L = L_2 - L_1$ and use the SP spectra after propagation of distance L_2 as the reference and the SP spectra after propagation of distance L_1 as the signal. The dominant process of SP decrease on the uncovered metal is the SP scattering into a free-space wave, which cannot be described by the formalism of this paper.

To find the optimal layer thickness for a particular application, we must distinguish the main processes occurring in this layered system. We start our investigation with the case when $d \ll \lambda$.

3.1. Thin films

An almost linearly dispersed (chirped) THz pulse is observed for a 20 μm film in the 0.2–1 THz range (figure 4(a)). Such a chirped pulse is a good criterion that indeed the SP but not a free-space wave is detected: the area of the layer (0.02×15 mm) is negligible for the cross-section of a free-space wave (15 mm $\times$ 15 mm) and the propagation of this wave cannot be significantly affected by such a thin film. Pulse stretching also confirms the high sensitivity of SP to the interface material—a transparent film of $d/\lambda \approx 0.03$ significantly changes the phase of the transmitted SP when the field is localized at the surface. Note that n_{SP} exceeds 1 only by 0.01 in this case (see figures 3(a) and 7(a)).

For the $d \ll \lambda$ case, the effective refractive index n_{SP} strongly depends on the wavelength and a short THz pulse is stretched in the time domain because of group velocity
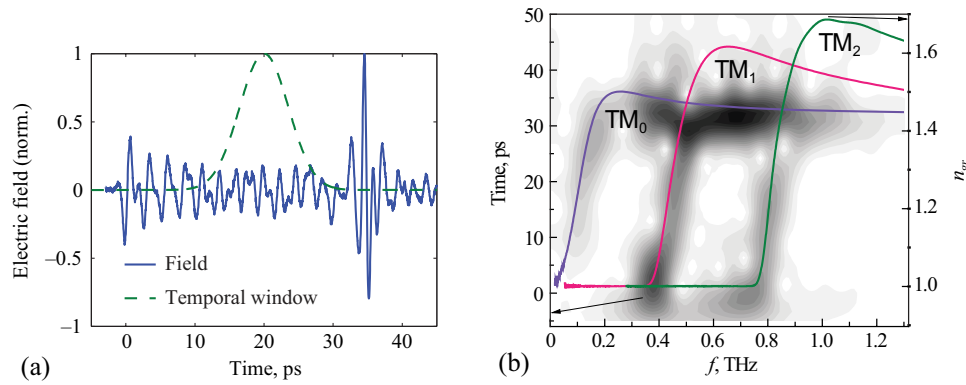
3

Figure 5. Pulse distortion due to the multimode regime for the dielectric layer with parameters $d = 370\ \mu$m, $L = 24$ mm. (a) SP pulse in the time domain and the temporal window centered at 20 ps. (b) Time–frequency representation for left vertical axis, planar waveguide mode group velocities are imposed on the plot with the right vertical axis.

dispersion (GVD) $\sim$d$^2 k_{SP}/$dω^2, where $k_{SP} = n_{SP}\omega/c$. The calculation of $n_{SP}(\omega)$ (see below) and correspondent GVD shows that the maximal (d$^2 k_{SP}/$d$\omega^2 \approx 800$ ps^2 cm^{-1}) pulse stretching occurs at $d/\lambda = 0.05-0.18$ and it decreases outside this range for both longer and shorter waves. Concavity of the $n(f)$ dependence (an indication that $\sim$d$^2 k_{SP}/$d$\omega^2 > 0$) can be seen on figure 2(a), for the $d = 20\ \mu$m case. Even a range of negative GVD can exist (at $d/\lambda \approx 1$) that could potentially compress chirped THz SP pulses.

The calculated field distribution (figure 4(b)) shows that the SP field is mostly localized in air (providing low material absorption) and at the same time the field is well confined to the surface ($\delta_z = 0.4$ mm at $f = 0.5$ THz).

Note that even thin transparent films may increase SP damping on flat and smooth surfaces [13, 14], because the transverse electric field profile of the plasmonic mode changes and losses in metal become more important. Hence, for a particular wavelength an optimal film thickness exists ($d/\lambda \approx 0.03$) for THz SP delivery over long distances.

3.2. Intermediate films

The most complicated is the 'middle' regime, when $d \approx \lambda \approx 300\ \mu$m. In this case, the slab supports not only SP modes but also the 'photonic' (planar waveguide) modes which are efficiently excited above its cut-off frequencies. As a result, many pulses emerge from the film (figure 5(a)) forming a complicated temporal and spectral shapes.

To visualize the excited modes separately, we plot a time–frequency representation [15] and observe localization of particular frequencies in the time domain. We multiply the initial signal by a Gaussian time window of 10 ps duration (figure 5(a)) and calculate a Fourier spectrum for each position of the window center, that is the time scale (left vertical axis) for a time–frequency plot in figure 5(b). More details about the time–frequency representation and THz SP can be found in [15]. Observed delay of a particular mode is determined by its correspondent group velocity. We calculated the so-called group refractive index, defined as $n_{gr} = n + \omega \partial n/\partial \omega$, of the first three modes using $n(\omega)$ extracted from equation (1) described below. Since the pulse delay (time scale) and group velocity are related through the waveguide length, we imposed n_{gr} spectra on figure 5(b). This gives an idea of each mode dispersion. For the fundamental (SP) mode, for frequencies above 0.2 THz $n_{gr} \approx$ const. That leads to a separate short pulse observed at $t = 35$ ps in figure 5(a). Besides the sample with the thickness of 370 μm, we observe similar multimode regime for the samples with $d = 200, 600, 750\ \mu$m. For larger d, the excitation efficiency of high order modes becomes very low, while for small d, the first (TM$_1$) mode cut-off frequency is higher than the SP maximal detectable frequency (1.2 THz). Calculated SP field distribution is an intermediate case between figures 4(b) and 6(b), in this case the SP field is partially localized inside the dielectric, and field confinement to the surface is not so good as for a thin film.

The measured total attenuation sharply increases above the TM$_1$ mode cut-off frequency. It is not correct to evaluate total refraction spectra in the traditional to THz-TDS manner for the multimode regime, since different modes interfere with each other. For the case of thick (200 and 750 mm) films, additional waveguide modes are removed from the temporal signal for the absorption and refraction spectra evaluation.

3.3. Thick films

For the $d \gg \lambda$ case, a part of the SP field is transformed into a free-space wave (at the front edge of the dielectric block) and propagates above the layer, see figure 6(a) at $t = 0$. Inside the layer, the SP pulse is considerably delayed and conserves short duration (see figure 6(a) at $t = 12$ ps). In this case SP does not interact with the upper interface and both SP localization and dispersion are low. The structure can be considered as a two-layer system with a dielectric instead of air with all the same disadvantages for THz range as for the initial metal–air interface. As a result, two short pulses come out of a thick dielectric block—a free-space wave and a delayed SP [10].

Calculated field distribution in figure 6(b) shows that the SP field is mainly localized inside the dielectric layer, hence the surface sensitivity is poor and material absorption becomes significant.
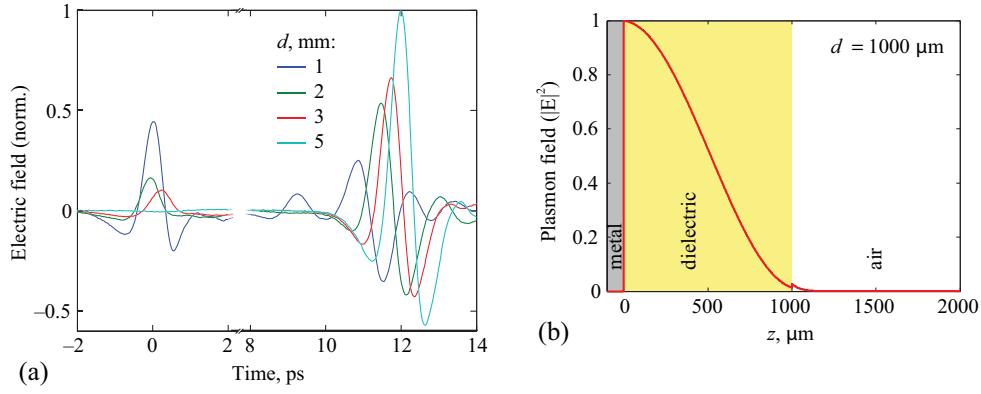
Figure 6. (a) Temporal shape of SP wave ($t > 10$ ps) and accompanied free-space wave ($t < 2$ ps) transmitted through thick ($d = 1$–5 mm) dielectric layers with $L = 8$ mm. (b) Field distribution for the $d = 1$ mm case.
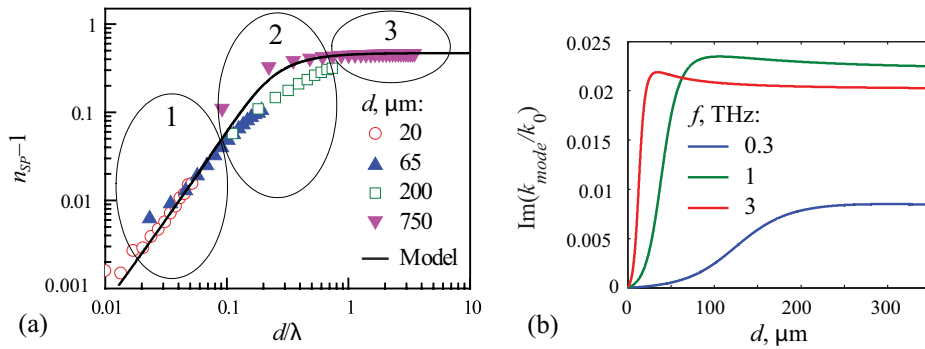

Figure 7. (a) Measured and calculated relative refractive index $n_{SP} - 1$ versus film thickness d normalized to the wavelength λ. (b) Calculated SP absorption (normalized imaginary part of the SP wavevector) versus film thickness for a set of frequencies.

For an undistorted pulse, we can extract the refraction directly from the time-domain data: $n = 1 + c\Delta t/L$, where Δt is the delay between reference and signal pulses. For $d = 1$ mm thickness we observe some dispersion and SP refraction index is still lower than the value for bulk dielectric, in the presented case ($L = 8$ mm, $\Delta t = 11$ ps) it is $n_{SP} = 1.41$, while for the $d = 5$ mm case no dispersion is observed and $\Delta t = 12$ ps, $n_{SP} = n_{bulk} = 1.44$.

The three different regimes of SP propagation through the block are theoretically analyzed below.

3.4. Theoretical analysis

We assumed that the main part of the energy upon SP transmission is coupled into a plasmonic mode supported by the metal surface covered with a dielectric film. The effective index $\beta = n_{SP}$, if such mode can be found from a well-known dispersion relation for the TM-polarized mode of the three-layer planar waveguide [1, 16]:

$$\tanh(\gamma_d d) = -\frac{\gamma_d \varepsilon_d (\varepsilon_a \gamma_m + \varepsilon_m \gamma_a)}{\varepsilon_a \varepsilon_m \gamma_d^2 + \varepsilon_d^2 \gamma_a \gamma_m}, \qquad (1)$$

where ε_m, ε_d, ε_a are the dielectric permittivities of the metal, dielectric film and surrounding dielectric (air), respectively, d is the thickness of the film, $\gamma_l = \beta^2 - k^2\varepsilon_l$, $l \in \{m, d, a\}$, $k = \omega/c$ (figure 1). Note that with an increase in d or ω this

equation has multiple roots corresponding to one plasmonic mode and several 'photonic' modes with the field distribution, similar to that of the usual TM-modes of a dielectric waveguide. Analytical estimations for limiting cases of d/λ for plasmonic and non-plasmonic modes for transparent dielectric can be found in [1, 3]. The huge value of the bulk metal–dielectric function ($\varepsilon_m \approx 10^4 + 10^5$i) makes the numerical solution of the transcendental equation (1) challenging. For the solution of the dispersion relation we use a stable iterative procedure similar to the one presented in [17].

It is known that in the case when the losses in the dielectric layer are relatively small, the plasmonic mode in such a structure exists at any layer thickness. When the layer thickness increases from 0, the propagation constant of the plasmonic mode also increases from the propagation constant of an SP at the metal–air interface to the propagation constant of an SP at the metal–dielectric interface. In the case of a transparent dielectric with low dispersion, the solution can be scaled with d or λ for the real part of SP wavevector k_{SP} (the same is valid for n_{SP} since $k_{SP} = n_{SP}\omega/c$), so $|k_{SP}(\lambda_1, d_1)/k_1| = |k_{SP}(\lambda_2, d_2)/k_2|$ if $d_1/\lambda_1 = d_2/\lambda_2$, hence $k_{SP}(d/\lambda)/k = n_{SP}(d/\lambda)$ function completely characterizes a three-layer system in a broad range of λ and d. Experimental data (with moderate absorption and dispersion in polymer materials) reasonably agrees with this scaling (figure 7(a)). For a more general scaling, one should use the value of

5

wavelength inside the dielectric film, i.e. make the following formal replacement: $\lambda \to \lambda/n_d$.

It is intuitively clear that the notation 'thick' and 'thin' should be related to the wavelength. So, for the values of $d/\lambda < 0.1$ we are in regime of thin films with strong dispersion (maximal GVD corresponds to $d/\lambda = 0.05 - 0.18$), for $d/\lambda \approx 1$ it is the intermediate case with increased SP absorption and a multimode regime, and for $d/\lambda \gg 1$ it is regime of thick films without dispersion ($n_{\text{SP}} \approx n_d \approx \text{const}$) and, again, with poor localization. Those three regimes are indicated in figure 7. Convexity of $n(f \sim 1/\lambda)$ dependence (indication that $\sim \mathrm{d}^2 k_{\text{SP}}/\mathrm{d}\omega^2 < 0$) can be seen in figure 7(a) for the region where d/λ is in the range 0.3–1. Let us note that the discrepancies between the experimental data and theoretical curve visible in region 2 in figure 7(a) mean that the phase of the transmitted signal in this case is determined not only by the SP but also by other modes in the multimode regime.

For the imaginary part of k_{SP} ($\text{Im}(k_{\text{SP}}) = \alpha_{\text{SP}}$), which determines the absorption coefficient of SP for propagation in the x direction, the situation is more complicated. There is no simple invariant of the form $\alpha_{\text{SP}}(\lambda_1, d_1) = \alpha_{\text{SP}}(\lambda_2, d_2)$, but still the film thickness $d_{\max}$ of maximal absorption $d_{\max} = \lambda/[4\sqrt{n_d^2 - 1}]$ [13] can be linearly scaled with the wavelength.

It is evident from figure 7(a) that, at a fixed frequency, it is possible to find the thickness value d that provides the given value of the propagation constant $\beta = kn_{\text{SP}}$ of the plasmonic mode, however, the relatively strong SP dispersion at 'small' thickness has to be taken into account. Obviously, it is the propagation constant of the mode that determines the γ_j values in (1), and, consequently, the penetration depth δ_z. The penetration depth into the dielectric is the one that should be minimized for the THz plasmonic modes [16] designed for surface sensitivity. As mentioned above, as a localization measure, an analogue of the penetration depth of an SPP into homogeneous dielectric was chosen, namely, the distance at which the field amplitude (e.g. the amplitude of the continuous **H** field) decreases by a factor of e (figure 1). It should be noted that in the general case the field maximum of the plasmonic mode is not necessarily located at the interface between the metal and the dielectric layer, so the resulting localization measure is considered as a sum of two values: the distance from the interface to the field amplitude maximum (typically, less then 1 μm) and the distance corresponding to an e times decay of the field. The dependences of this localization measure on the layer thickness for a set of frequencies are shown in figure 8. For each frequency, a value of d that provides the minimum value of the localization measure (i.e. the minimum penetration depth) can be found. In the 0.3–1 THz range this value is between 100 and 10 μm for common polymers with $n_d = 1.4$–1.5.

We estimate that for a broadband THz pulse a LDPE film of 10–30 μm height is a reasonable compromise between dispersion and absorption on the one hand and poor confinement and radiation losses on the other hand.
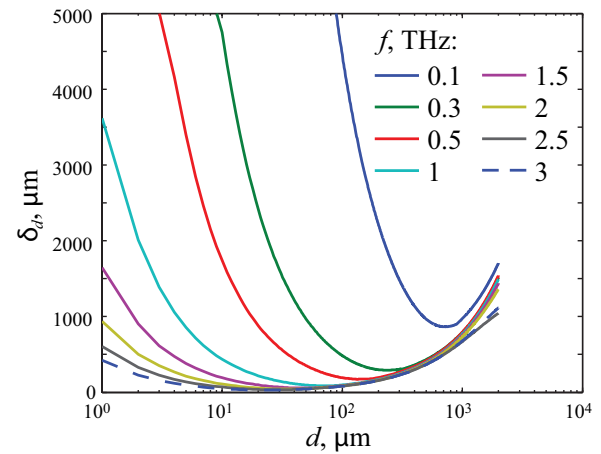

Figure 8. SP localization δ_d versus film thickness d for a set of frequencies indicated in the legend in THz.

4. Conclusion

In the present work, transmission of broadband THz SP pulses through dielectric slabs with different thickness d was experimentally studied and theoretically analyzed. It was demonstrated that the temporal and spectral shapes of the transmitted SP pulses differ considerably for the three established regimes of plasmon–layer interaction: $d \ll \lambda$, $d \approx \lambda$ and $d \gg \lambda$. It was shown that a thin ($d \approx \lambda/30 \approx 10$ μm) dielectric film on the metal surface considerably enhances SP localization without introducing much dispersion and absorption. The most transparent polymers with absorption coefficient $\alpha < 0.5$ cm^{-1} will lead to SP propagation lengths on the order of 10 cm, with 1 mm localization. Films of intermediate thickness ($d \approx \lambda$) may support a set of waveguide modes at specific frequencies together with a broadband SP. Thick films preserve short pulse shape.

Using the approach developed here, it is possible to control surface confinement, to deliver THz SP over long distances, and to stretch short pulses. Such SP features as field localization (local field enhancement, selective sensitivity to surface) and propagation (large interaction length, guiding to a surface) determine its potential for applications in the THz spectroscopy of thin films and signal processing.

References

Q.3

[1] Sannikov D G and Sementsov D I 2003 *Tech. Phys. Lett.* **29** 353
[2] Avrutsky I, Soref R and Buchwald W 2010 *Opt. Express* **18** 348

[3] Bezus E A, Doskolovich L L and Kazanskiy N L 2011 *Appl. Phys. Lett.* **98** 221108

[4] Lo S-Z A and Murphy T E 2010 *Appl. Phys. Lett.* **96** 201104

[5] Gong M, Jeon T-I and Grischkowsky D 2009 *Opt. Express* **17** 17088

[6] Nazarov M, Coutaz J-L, Shkurinov A and Garet F 2007 *Opt. Commun.* **277** 33

[7] Barnes W L 2006 *J. Opt. A: Pure Appl. Opt* **8** S87

[8] Nazarov M M, Shkurinov A P, Angeluts A A and Sapozhnikov D A 2009 *Radiophys. Quantum Electron.* **52** 536

[9] Agranovich V M and Mills D L 1982 *Surface Polaritons* (Amsterdam: North-Holland, American Elsevier) p 123

[10] Nazarov M M, Shkurinov A P, Ryabov A Y and Bezus E A 2010 *IRMMW-THz2010, Technical Digest on CD* We-P.47

[11] Lee Y-S 2009 *Principles of Terahertz Science and Technology* Springer Science+Business Media, LLC p 234

[12] Fedulova E V, Nazarov M M, Angeluts A A, Kitai M S, Sokolov V I and Shkurinov A P 2012 *Proc. SPIE* **8337** 83370I

[13] Zhizhin G N, Nikitin A K, Bogomolov G D, Zavialov V V, Uk J U, Cheol J B, Park S H and Cha H J 2006 *Opt. Spectrosc.* **100** 734

[14] Gerasimov V V, Knyazev B A and Nikitin A K 2010 *Vestn. Novosibirsk State Univ. Ser.: Phys.* **5** 158

[15] Nazarov M M, Mukina L S, Shuvaev A V, Sapozhnikov D A, Shkurinov A P and Trofimov V A 2005 *Laser Phys. Lett.* **2** 471

[16] Bezus E A, Doskolovich L L, Kazanskiy N L and Soifer V A 2011 *Tech. Phys. Lett.* **37** 1091

[17] Kekatpure R D, Hryciw A C, Barnard E S and Brongersma M L 2009 *Opt. Express* **17** 24112

Q.4

Q.5

Q.6